Research Article | Vol. 26, No. 9 | 30 Apr 2018 | OPTICS EXPRESS 12049
Optics EXPRESS

Optimum repetition rates for dual-comb spectroscopy

Brad C. Smith,* Bachana Lomsadze, and Steven T. Cundiff

Department of Physics, University of Michigan, Ann Arbor, MI 48109, USA
bradcs@umich.edu

Abstract: The determination of the properties (i.e. line center, width, and amplitude) of a spectral line is simulated using a Monte Carlo method. For dual-comb spectroscopy, ideal repetition rates emerge for both the signal and LO combs that do *not* correspond to the repetition rates that possess the highest signal-to-noise ratio. The determination is even more accurate when the repetition rates have an arbitrary near-harmonic ratio. The simulation results are generalized to allow for the comparison of any two spectroscopic systems (i.e. not just comb-based systems) by performing the simulations as a function of the spectral point spacing and signal-to-noise ratio of the acquired data.

OCIS codes: (300.0300) Spectroscopy; (300.6360) Spectroscopy, laser; (280.0280) Remote sensing and sensors.

References and links

1. S. T. Cundiff and J. Ye, "Colloquium: Femtosecond optical frequency combs," Rev. Mod. Phys. **75**, 325–342 (2003).
2. S. A. Diddams, "The evolving optical frequency comb [Invited]," J. Opt. Soc. Am. B **27**, B51–B62 (2010).
3. I. Coddington, N. Newbury, and W. Swann, "Dual-comb spectroscopy," Optica **3**, 414 (2016).
4. T. Ideguchi, "Dual-Comb Spectroscopy," Opt. Photon. News **28**, 32–39 (2017).
5. N. R. Newbury, I. Coddington, and W. Swann, "Sensitivity of coherent dual-comb spectroscopy," Opt. Express **18**, 7929–7945 (2010).
6. B. Bernhardt, A. Ozawa, P. Jacquet, M. Jacquey, Y. Kobayashi, T. Udem, R. Holzwarth, G. Guelachvili, T. W. Hänsch, and N. Picqué, "Cavity-enhanced dual-comb spectroscopy," Nat. Photonics **4**, 55–57 (2010).
7. I. Coddington, W. C. Swann, and N. R. Newbury, "Coherent dual-comb spectroscopy at high signal-to-noise ratio," Phys. Rev. A **82**, 1–13 (2010).
8. G. Millot, S. Pitois, M. Yan, T. Hovhannisyan, A. Bendahmane, T. W. Hänsch, and N. Picqué, "Frequency-agile dual-comb spectroscopy," Nat. Photonics **10**, 27–30 (2015).
9. A. Nishiyama, S. Yoshida, T. Hariki, Y. Nakajima, and K. Minoshima, "Sensitivity improvement of dual-comb spectroscopy using mode-filtering technique," Opt. Express **25**, 31730–31738 (2017).
10. M. A. Duguay and J. W. Hansen, "Optical sampling of subnanosecond light pulses," Appl. Phys. Lett. **13**, 178–180 (1968).
11. J. Davila-Rodriguez, M. Bagnell, C. Williams, and P. J. Delfyett, "Multiheterodyne Detection for Spectral Compression and Downconversion of Arbitrary Periodic Optical Signals," J. Light. Technol. **29**, 3091–3098 (2011).
12. A. Klee, J. Davila-Rodriguez, C. Williams, and P. J. Delfyett, "Characterization of semiconductor-based optical frequency comb sources using generalized multiheterodyne detection," IEEE J. Sel. Top. Quantum Electron. **19** (2013).
13. N. B. Hébert, S. Boudreau, J. Genest, and J.-D. Deschênes, "Coherent dual-comb interferometry with quasi-integer-ratio repetition rates," Opt. Express **22**, 29152–29160 (2014).
14. L. Antonucci, X. Solinas, A. Bonvalet, and M. Joffre, "Asynchronous optical sampling with arbitrary detuning between laser repetition rates," Opt. Express **20**, 17928 (2012).
15. D.-S. Ly-Gagnon, S. Tsukamoto, and K. Katoh, "Coherent Detection of Phase-Shift Keying Signals Using Digital Carrier-Phase Estimation," J. Light. Technol. **24**, 12–21 (2006).
16. I. Coddington, F. R. Giorgetta, E. Baumann, W. C. Swann, and N. R. Newbury, "Characterizing fast arbitrary cw waveforms with 1500 thz/s instantaneous chirps," IEEE J. Sel. Top. Quantum Electron. **18**, 228–238 (2012).
17. E. Baumann, F. R. Giorgetta, W. C. Swann, A. M. Zolot, I. Coddington, and N. R. Newburry, "Spectroscopy of the Methane ν_3 Band with an Accurate Mid-Infrared Coherent Dual- Comb Spectrometer," Phys. Rev. A **84**, 062513 (2011).
18. Y.-D. Hsieh, Y. Iyonaga, Y. Sakaguchi, S. Yokoyama, H. Inaba, K. Minoshima, F. Hindle, T. Araki, and T. Yasui, "Spectrally interleaved, comb-mode-resolved spectroscopy using swept dual terahertz combs," Sci. Rep. **4**, 1–7 (2014).
19. T. Ideguchi, S. Holzner, B. Bernhardt, G. Guelachvili, N. Picqué, and T. W. Hänsch, "Coherent raman spectro-imaging with laser frequency combs," Nature. **502**, 355 (2013).

#319042 https://doi.org/10.1364/OE.26.012049
Journal © 2018 Received 5 Jan 2018; revised 2 Mar 2018; accepted 13 Mar 2018; published 26 Apr 2018

Optics EXPRESS

20. B. Lomsadze and S. T. Cundiff, "Frequency comb-based four-wave-mixing spectroscopy," Opt. Lett. **42**, 2346–2349 (2017).
21. B. Lomsadze and S. T. Cundiff, "Frequency combs enable rapid and high-resolution multidimensional coherent spectroscopy," Science. **357**, 1389–1391 (2017).
22. B. Lomsadze and S. T. Cundiff, "Multi-heterodyne two dimensional coherent spectroscopy using frequency combs," Sci. Reports **7**, 14018 (2017).
23. A. Asahara and K. Minoshima, "Development of ultrafast time-resolved dual-comb spectroscopy," APL Photonics **2**, 041301 (2017).
24. K. J. Mohler, B. J. Bohn, M. Yan, G. Mélen, T. W. Hänsch, and N. Picqué, "Dual-comb coherent Raman spectroscopy with lasers of 1-GHz pulse repetition frequency," Opt. Lett. **42**, 318–321 (2017).
25. J.-D. Deschênes and J. Genest, "Heterodyne beats between a continuous-wave laser and a frequency comb beyond the shot-noise limit of a single comb mode," Phys. Rev. A **87**, 023802 (2013).
26. M.-G. Suh, Q.-F. Yang, K. Y. Yang, X. Yi, and K. J. Vahala, "Microresonator soliton dual-comb spectroscopy," Science **354**, 600–603 (2016).
27. T. J. Kippenberg, R. Holzwarth, and S. A. Diddams, "Microresonator-Based Optical Frequency Combs," Science **332**, 555–559 (2011).
28. T. O'Haver, *A Pragmatic Introduction to Signal Processing: with applications in scientific measurement* (CreateSpace Independent Publishing Platform, 2016), 2nd ed.
29. J. Chen, J. W. Sickler, P. Fendel, E. P. Ippen, F. X. Kärtner, T. Wilken, R. Holzwarth, and T. W. Hänsch, "Generation of low-timing-jitter femtosecond pulse trains with 2 GHz repetition rate via external repetition rate multiplication," Opt. Lett. **33**, 959–961 (2008).
30. M. S. Kirchner, D. A. Braje, T. M. Fortier, A. M. Weiner, L. Hollberg, and S. A. Diddams, "Generation of 20 GHz, sub-40 fs pulses at 960 nm via repetition-rate multiplication," Opt. Lett. **34**, 872–874 (2009).
31. L. Yang, H. Yang, H. Zhang, H. Wei, and Y. Li, "Repetition rate multiplication of frequency comb using all-pass fiber resonator," Rev. Sci. Instruments **87**, 093101 (2016).

1. Introduction

Frequency combs have revolutionized the fields of spectroscopy and optical frequency metrology over the past few decades due to their long coherence times, high precision, and ability to create a direct link between optical and microwave frequencies [1]. This impact has been felt in a diversity of areas from attosecond science to tests of fundamental physics to even exoplanetary science [2]. For spectroscopy in particular, the unique combination of high precision and fast acquisition time enabled by dual-comb spectroscopy (DCS) has challenged Fourier Transform Infrared Spectroscopy (FTIR) - the longtime gold standard of high-resolution broadband spectroscopy [3]. DCS has proven to be highly proficient at identifying and measuring the concentrations of molecules, which is desirable for a variety of applications such as greenhouse gas sensing, toxin detection, and biomedical tissue analysis [4]. To succeed in these endeavors, it is imperative to be able to accurately and precisely measure the properties (i.e. line center, width, and amplitude) of some spectral feature. Of course the speed and accuracy of this task benefit from a higher signal-to-noise ratio (SNR); the understanding and improvement of which have been the focus of many previous works [5–9]. However, the SNR is not the only significant parameter – as we show in this work, the repetition rates of the two combs have a tremendous impact on the error and uncertainty of the ascertained line properties assuming all else is equal. This impact is greatest when allowing for the selection of arbitrary-harmonic related repetition rates.

In the conventional implementation of DCS, one comb (referred to as the signal comb with a repetition rate of f_{Sig}) is transmitted through a medium of interest while the second comb (referred to as the local oscillator (LO) or "read-out" comb with a repetition rate of f_{LO}) bypasses the medium and interferes with the signal comb on a detector. The repetition rates of the two combs are slightly different so that their ratio ($\rho_{\mathrm{r}} \equiv f_{\mathrm{LO}} : f_{\mathrm{Sig}}$) is very close to unity. In the frequency-domain, this ratio means that the beat notes between any two signal and LO comb lines seen on the detector occur at unique, evenly spaced frequencies thereby forming a radio-frequency (rf) comb. This one-to-one mapping links the measured rf comb lines and the optical comb lines that generated them. Because the amplitude and phase of each individual signal comb line can be measured, the spectral line is sampled with a spectral point spacing, $\delta\nu$, equal to

Optics EXPRESS

f_{Sig}. In the time-domain, the use of nearly identical repetition rates implies that the time delay between sequential pairs of signal and LO pulses increases by a small, very precise amount. This configuration is analogous to FTIR in the sense that the relative time-delay between two pulses is scanned so that they sample one another at discrete points and indeed the recorded interferograms appear very similar. However, by taking advantage of the high precision of combs and avoiding the use of a mechanical delay stage, DCS has significantly better spectral resolution, compactness, robustness, and acquisition times.

Although the repetition rates of the two combs used in the vast majority of conventional DCS setups possess a near-unity ratio, in principle any near-harmonic (i.e. near-multiple) relationship between the repetition rates is acceptable. The concept of heterodyning two periodic optical waveforms with arbitrary near-harmonic repetition rates has been used to characterize the envelope [10] and more recently the envelope and spectral phase [11, 12] of an unknown waveform. The latter two techniques are quite similar to DCS in the way that they retrieve optical information from the rf signal by leveraging the one-to-one mapping between a pair of signal and LO comb lines and their beat note on a detector. The use of near-harmonic repetition rate combs has also been applied to DCS – but rather than directly using the rf-to-optical mapping, the authors viewed the measured rf signal as a temporal-multiplexing of independent traditional DCS interferograms then demultiplexed and combined them [13]. Another method that utilizes two pulse trains actually allows for *any* ρ_{r} although its sub-picosecond time accuracy is insufficient for DCS [14].

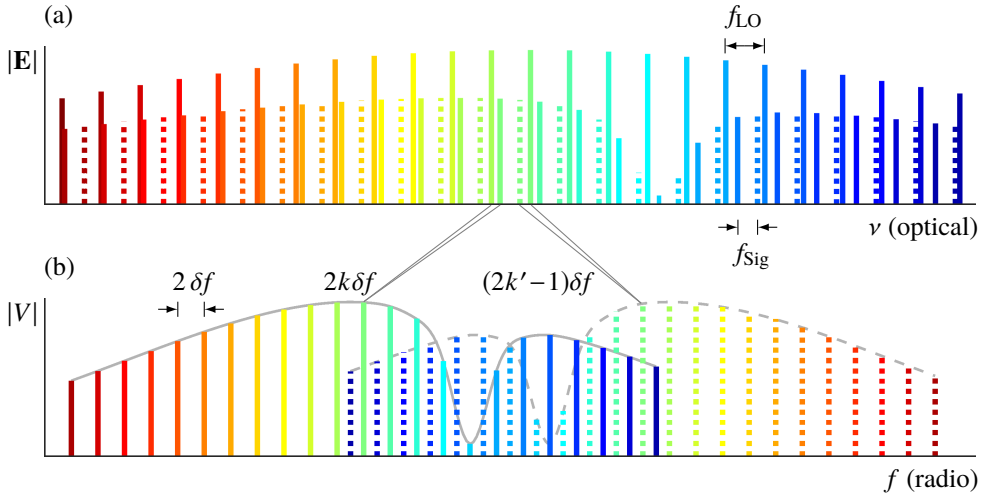

Fig. 1. (a) Optical spectra of a signal comb (showing an absorption dip) and LO comb with equal average powers and a repetition rate ratio $\rho_{\mathrm{r}} \approx 2:1$. Every other signal comb line is dotted to illustrate where the rf comb lines in (b) originate. (b) The rf comb seen on a detector in an electrical bandwidth of $f_{\mathrm{LO}}/2$. A pair of gray lines illustrates the optical-to-rf mapping for a solid (dotted) rf comb line which in this specific example occur at even (odd) multiples of δf (k and k' are integers). Note that each "interferogram" in the time-domain will contain two unique bursts (corresponding to the solid and dotted rf combs) because the LO pulse train sweeps through a given signal pulse twice during each $\tau_{\mathrm{min}} \equiv \delta f^{-1}$.

An example of how the optical information is mixed into the rf domain on a detector for ρ_{r} near $2:1$ is shown in Fig. 1. From Fig. 1 it is clear that the maximum optical bandwidth, $\Delta\nu_{\mathrm{max}}$,

Optics EXPRESS

that can be used without ambiguity is

$$\Delta\nu_{\max} = \frac{f_{\mathrm{Sig}} f_{\mathrm{LO}}}{2\,\delta f} \quad , \tag{1}$$

where the required rf point spacing is

$$\delta f = \begin{cases} \left| \frac{f_{\mathrm{LO}}}{\mathrm{nint}\left(\rho_{\mathrm{r}}\right)} - f_{\mathrm{Sig}} \right|, & \rho_{\mathrm{r}} > 1 \\ \left| f_{\mathrm{LO}} - \frac{f_{\mathrm{Sig}}}{\mathrm{nint}\left(\rho_{\mathrm{r}}^{-1}\right)} \right|, & \rho_{\mathrm{r}} < 1 \end{cases} \tag{2}$$

where $\mathrm{nint}(x)$ is the nearest integer function. Note that the necessary rf point spacing is equal to the difference between the repetition rates for only conventional DCS (where $\rho_{\mathrm{r}} \approx 1$). The maximum optical bandwidth can be doubled by using in-phase/quadrature detection [15, 16]. The minimum amount of time required to resolve these rf comb teeth is $\tau_{\min} \equiv \delta f^{-1}$ as set by the Nyquist criterion. Once resolved, the desired optical information can be extracted from the rf comb [11–13].

2. Simulation

The impact of various experimental parameters on the determination of the properties (i.e. line center, width, and amplitude) of some spectral feature can be quantified using a Monte Carlo method. Many randomly generated data sets with appropriate SNRs are each fit using a regression approach to extract the properties of the spectral feature. The errors between these measured values and the ones used to generate the data are then analyzed as a function of the experimental parameter to reveal its influence.

A number of approximations and assumptions have been made to simplify our analyses. First, we only consider a sample medium that possesses a single Lorentzian resonance and only analyze the absorption due to this resonance i.e. phase information is neglected. Second, we approximate the spectral envelopes of the signal and LO pulse trains as "top hats" whose width, $\Delta\nu$, is less than $\Delta\nu_{\max}$. In Sec. 2.1 the amplitude of the top hat is such that the average power of each beam is fixed while in Sec. 2.2 it is irrelevant. Third, the response function of the detector is assumed to be flat and the rf comb (which we assume lines up perfectly with the measurement frequency grid) is sampled at a rate of f_{LO}. Fourth, we assume that the offset frequency and repetition rate noise of the combs is negligible and that the dominant noise in the measurement may be modeled as additive complex white Gaussian noise, $N(\nu)$. Fifth, we assume that all systematic errors (e.g. baseline issues from etalon effects) are negligible.

These assumptions allow us to write the normalized, dimensionless, noise-free, optical-domain signal as

$$S(\nu) = \exp\left[2\pi i\, n'(\nu)\, L\nu/c\right] \exp\left[-\alpha(\nu)\, L/2\right] \quad , \tag{3}$$

which is only sampled at the signal comb frequencies within $\Delta\nu$ given by $\nu = k\, f_{\mathrm{Sig}} + f_{\mathrm{o}}$ where k is an integer, f_{o} is the signal comb offset frequency, $n'(\nu)$ is the real part of the sample medium's refractive index and L its length, and the absorption coefficient is

$$\alpha(\nu) = \frac{s}{L}\, \frac{\gamma^2}{\gamma^2 + (\nu - \nu_{\mathrm{c}})^2} \quad . \tag{4}$$

The parameters to be obtained from the noisy data are the center frequency, ν_{c}, half-width at half maximum (HWHM), γ, and the strength, s. Since the phase information is neglected in this work, the noisy signal is

$$S_N(\nu) \equiv \left| S(\nu) + N(\nu) \right| \quad , \tag{5}$$

Optics EXPRESS

in which we expect the average SNR for a weakly absorbing sample to be

$$\mathrm{SNR}_{\rho_\mathrm{r}} = \sqrt{\rho_\mathrm{r}}\,\mathrm{SNR}_1 \tag{6}$$

where the corresponding SNR for conventional (i.e. $\rho_\mathrm{r} \approx 1$) DCS is [5]

$$\mathrm{SNR}_1 \equiv \frac{\sqrt{\tau}}{M}\frac{2P_\mathrm{Sig}}{\left[\mu^{-1}\,(\mathrm{NEP})^2 + 4c_1\eta^{-1}h\nu_0 P_\mathrm{Sig} + 2bc_2\,(\mathrm{RIN})\,P_\mathrm{Sig}^2\right]^{1/2}} \quad , \tag{7}$$

where τ is the acquisition time, $M \equiv \Delta\nu/f_\mathrm{Sig}$ is the number of resolved spectral elements (where $\Delta\nu$ is the acquisition optical bandwidth), P is the average laser power incident on the detector, NEP and η are the noise equivalent power and efficiency of the detector respectively, $\mu \equiv P_\mathrm{LO}/P_\mathrm{Sig}$ is the laser power ratio, $h\nu_0$ is the average energy per photon, $c_1 \equiv (1+\mu)/(2\mu)$, $c_2 \equiv (1+\mu^2)/(2\mu)$, b is 1 (2) for balanced (unbalanced) detection, and RIN is the laser relative intensity noise (assumed to be the same for both pulse trains). Eq. (7) does not contain the factor of 0.8 found in Ref. [5] because the laser spectra are assumed to be "top-hats" rather than Gaussians. From a frequency-domain perspective, the SNR expression in Eq. (6) arises from the facts that ρ_r more interferograms can be measured for any given τ and $\Delta\nu$ per Eqs. (1) and (2) (increasing the SNR by $\sqrt{\rho_\mathrm{r}}$ due to averaging), the amplitudes of the LO comb lines are $\sqrt{\rho_\mathrm{r}}$ times larger, and the frequency domain noise amplitude increases by $\sqrt{\rho_\mathrm{r}}$ because the sampling rate increases by ρ_r. In the time-domain, the same $\sqrt{\rho_\mathrm{r}}$ benefit from averaging and the same $\sqrt{\rho_\mathrm{r}}$ times greater noise amplitude from faster sampling exist in addition to a LO electric field amplitude that is $\sqrt{\rho_\mathrm{r}}$ greater on average.

2.1. Varying the repetition rates

For a fair comparison of repetition rates to be used in DCS, all other experimental parameters are fixed. In this case, Eq. (6) implies that the SNR scales with the repetition rates as

$$\mathrm{SNR} \propto \sqrt{f_\mathrm{Sig} f_\mathrm{LO}} \quad , \tag{8}$$

as shown in the leftmost panel of Fig. 2. Eq. (8) has recently been experimentally verified in Ref. [9] (note the reported SNRs are for the rf power as opposed to amplitude – the latter being the convention used in this work). For any given signal and LO comb repetition rates, the noisy signal $S_N(\nu)$ from Eq. (5) (with $L = 1$ and $s = 1$) was simulated independently many times with a SNR given by Eq. (8) and a random signal comb offset frequency, f_o, each time. Then, for each simulation, $-2\ln[S_N(\nu)]/L$ was fit to Eq. (4) using a nonlinear least-squares method following the Levenberg-Marquardt algorithm. The standard deviation of the errors in the fitted center frequency (σ_c), HWHM (σ_γ), and strength (σ_s) were then recorded and are displayed in the rightmost three panels of Fig. 2.

In DCS the spectral point spacing, $\delta\nu$, is usually equal to the signal comb repetition rate, f_Sig. However, it is possible to achieve the same spectral point spacing with a signal comb repetition rate that is m times greater (where m is an integer) by using the spectral interleaving technique in which a series of m separate spectra are collected with each one having shifted signal comb lines [17, 18]. According to Eqs. (6) and (7) the SNR in the final interleaved spectrum is identical to one acquired without interleaving because the increase in the signal comb repetition rate by a factor of m (increasing the SNR by a factor $\sqrt{m}$) is counteracted by the reduction in acquisition time allowed for each measurement by a factor of m (decreasing the SNR by a factor $1/\sqrt{m}$) assuming all other parameters are the same. Thus, the results in Fig. 2 also apply to systems using the spectral interleaving technique but with the understanding that the horizontal axis should be interpreted as the final spectral point spacing, $\delta\nu$, which is f_Sig/m.

Optics EXPRESS

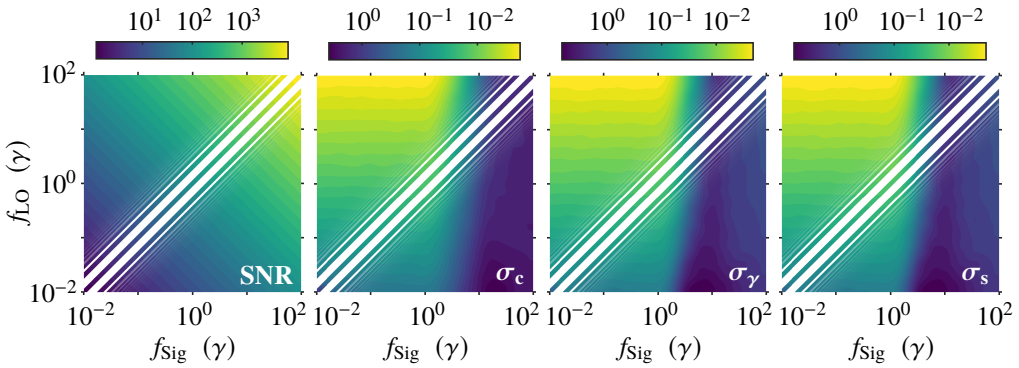

Fig. 2. SNR and corresponding standard deviations of the errors in the fitted center frequency (σ_c), HWHM (σ_γ), and strength (σ_s) as functions of the repetition rates of the signal and LO combs (which have units of γ, the HWHM of the resonance). Conventional ($\rho_r \approx 1$) DCS is the middle diagonal line on each plot while the first line above (below) the diagonal corresponds to $\rho_r \approx 2$ ($\rho_r^{-1} \approx 2$) and so forth. The space between neighboring lines shrinks exponentially due to the logarithmic axes.

The core result of this work is that the repetition rates of the signal and LO combs greatly impact the error and uncertainty in the measured parameters of a Lorentzian resonance which is clearly shown in Fig. 2. When all other experimental parameters are fixed, it is ideal to have $f_{Sig} \approx f_{LO} \approx \gamma$ when using the traditional implementation of DCS in which $\rho_r \approx 1$. However, by allowing the repetition rates to have a near-harmonic relationship, the uncertainty in the fit parameters can be orders of magnitude lower (assuming $f_{Sig} \lessapprox \gamma$) resulting from an SNR that scales with $\sqrt{\rho_r}$ (see Eq. 6 and the following paragraph). In this case, it is ideal to have any $f_{Sig} \lessapprox \gamma$ in addition to the highest near-harmonic LO repetition rate that is feasible. Of course there is a lower limit set on the signal comb repetition rate that corresponds to the SNR approaching 1. Note that it is never beneficial to use a near-subharmonic LO comb as can be seen in Fig. 2 – this would imply that many signal pulses are never sampled, wasting potential data. Although any signal comb repetition rate below the HWHM of the resonance should produce nearly the same fitting error for a given f_{LO} (see Fig. 2), there may be practical reasons to choose one f_{Sig} over another. For example, the higher the signal comb repetition rate, the less congested the rf comb will be because there are fewer comb teeth in a given electrical bandwidth. On the other hand, the higher the signal comb repetition rate, the less versatile that system will be in the sense that fewer samples will meet the $f_{Sig} \lessapprox \gamma$ requirement.

It is important to note that these results apply strictly to linear measurements because Eq. (3) does not accurately describe nonlinear signals in general. For example, nonlinear interactions typically generate new comb lines rather than attenuate existing ones [19–23]. Indeed one nonlinear experiment demonstrated that the SNR actually decreases with increasing f_{Sig} (fixed laser output powers), which would imply that lower signal comb repetition rates are always better for nonlinear measurements due to the higher energy per pulse [24]. Of course there are other techniques that can affect the SNR even for linear measurements. For instance, the GATOR technique can be used, which would favor a slower LO comb [25].

2.2. *Varying the SNR and spectral point spacing*

The results of Sec. 2.1 isolate the advantage stemming from the use of near-harmonically related repetition rates. However, most practical DCS systems have sufficiently different laser powers, detector efficiencies, types of dominant noise, etc., such that a more general simulation approach is necessary. For example, DCS has recently been performed with microresonator combs [26],

Optics EXPRESS

but because these combs typically output only milliwatts of power [27], it is inappropriate to use the results from Fig. 2 to compare their ability to ascertain the properties of a spectral line to slower oscillators that have orders of magnitude more output power. To generalize our results, the simulations were performed again but instead of varying the repetition rates, the independent parameters selected were the SNR and the spectral point spacing, $\delta\nu$. In all other respects the simulation process was identical to that described in Sec. 2.1. The results are displayed in Fig. 3.

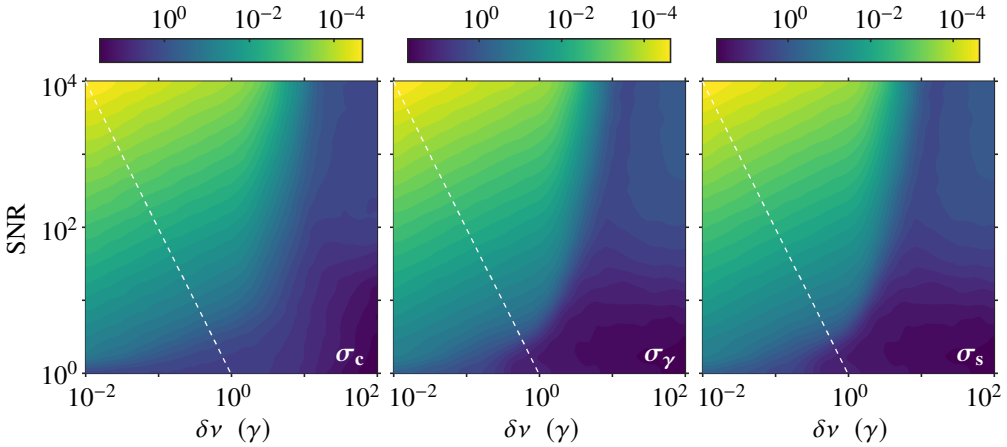

Fig. 3. Standard deviation of the errors in the fitted center frequency (σ_c), HWHM (σ_γ), and strength (σ_s) as functions of the SNR and spectral point spacing, $\delta\nu$. The dashed white lines are gradients to help illustrate the relationship in Eq. (9).

Examining the left-hand side of each plot in Fig. 3 reveals that as long as $\delta\nu \lessapprox \gamma$ and the SNR is sufficiently high, then

$$\sigma \propto \frac{\sqrt{\delta\nu}}{\mathrm{SNR}} \tag{9}$$

where σ is the standard deviation of a given fit parameter. This is a known result in signal processing that also applies to Gaussian and Voigt profile line shapes as well [28]. This result is completely general and not specific to DCS because the simulation merely fits a Lorentzian to arbitrarily collected data. Any two spectroscopic systems can be compared regardless of the laser power used, acquisition time, etc., as long as the sample is weakly absorbing and the noise is white, Gaussian distributed, and dominates the systematic error. Therefore, Eq. (9) provides a useful tool to compare any two spectroscopic systems. It also explains in Fig. 2 why σ_c, σ_γ, and σ_s, are all proportional to $1/\sqrt{f_{LO}}$ (with zero f_{Sig} dependence) for $f_{Sig} \lessapprox \gamma$ when one considers the SNR expression in Eq. 8 and the fact that $\delta\nu = f_{Sig}$.

All of the plots in Figs. 2 and 3 show that the error rapidly climbs for $\delta\nu \gtrapprox 3\gamma$. This observation corroborates one's intuition because zero (or only one) signal comb lines are "hitting the resonance." This condition means that the vast majority of the fitting involves the wings of the Lorentzian which are inherently insensitive to changes in ν_c, γ, and d (i.e. a large change in one of the parameters results in a minuscule change in data points far from line center) due to the exponential behavior of the wings. This lack of sensitive data points quickly leads to huge uncertainty in the fitted parameters *despite the fact that the* SNR *monotonically increases with* f_{Sig} (and therefore $\delta\nu$).

To verify the comprehensiveness of the results in Figs. 2 and 3 several series of simulations were performed. First, the overall patterns in the error plots remained the same as the SNR was scaled up and down over several orders of magnitude. Second, the number of data points

Optics EXPRESS

over which the fitting was performed was varied between a fixed number of data points, a fixed frequency range of data points, and a hybrid approach. There was no significant effect on our results. Third, the strength of the resonance was varied. For sufficiently small strengths ($s \lessapprox 5$) the general patterns in our results were unaffected. However, for larger strengths the absorption becomes saturated and the comb lines containing the most critical information (those near line center) have drastically reduced signal-to-noise ratios. This situation leads to significantly less accurate fits overall.

3. Conclusion

We have isolated the impact of the DCS comb repetition rates on the standard deviation of the error, σ, of the measured parameters of a single Lorentzian resonance (assuming all else is equal, i.e. lasers powers, acquisition time, etc.) and found that there is a maximum suitable spectral point spacing, $\delta\nu \approx \gamma$, where γ is the HWHM of the resonance. Because of this, the repetition rates that yield the smallest errors in the fit parameters do *not* possess the highest SNR. For the traditional implementation of DCS the ideal repetition rates are $f_{\mathrm{Sig}} \approx f_{\mathrm{LO}} \approx \gamma$ but even more accurate measurements can be made by allowing for arbitrary near-harmonic repetition rate ratios. In this case the ideal repetition rates are $f_{\mathrm{Sig}} \lessapprox \gamma$ and $f_{\mathrm{LO}} \to \infty$. In general, $\sigma \propto 1/\sqrt{f_{\mathrm{LO}}}$ (with zero f_{Sig} dependence) for $f_{\mathrm{Sig}} \lessapprox \gamma$. These are timely results given the recent advances in high-repetition-rate microresonator combs [26] and external repetition rate multiplying techniques [9, 29–31]. Since utilizing near-harmonic repetition rates requires only a slight modification to the rf-to-optical mapping process, any application of DCS where measuring the parameters of a spectral line is a top priority should readily receive higher accuracy and lower uncertainty by switching from similar to near-harmonic repetition rates assuming other experimental parameters remain more or less unchanged.

In practice, spectroscopic systems may differ wildly in everything from the type of dominant noise to the maximum allowable acquisition time. By running our simulations as a function of the SNR and spectral point spacing, $\delta\nu$, we identified a general fitting result, $\sigma \propto \sqrt{\delta\nu}$ / SNR, which can be used to compare any two spectroscopic systems despite their differences. In fact, this relationship can be used to compare even non-comb-based systems as long as the noise is predominately white and Gaussian distributed. Such a metric shows that while the SNR is important, efforts to reduce the spectral point spacing should also be made.

Funding

National Science Foundation (NSF) (1256260); Intelligence Advanced Research Projects Activity (IARPA) (2016-16041300005).

Acknowledgments

The authors extend their gratitude to Eric Martin for useful discussions. This research is based on work supported by the Office of the Director of National Intelligence (ODNI), Intelligence Advanced Research Projects Activity (IARPA), via contract 2016-16041300005. The views and conclusions contained herein are those of the authors and should not be interpreted as necessarily representing the official policies or endorsements, either expressed or implied, of the ODNI, IARPA, or the U.S. government. The U.S. government is authorized to reproduce and distribute reprints for governmental purposes notwithstanding any copyright annotation thereon.